

Strengthening of a Bridge Using Two FRP Technologies

Paolo Casadei, Nestore Galati, Renato Parretti and Antonio Nanni

Synopsis

This paper reports on the use of externally bonded fiber reinforced polymers (FRP) laminates and Near Surface Mounted FRP bars for the flexural strengthening of a concrete bridge. The bridge selected for this project is a three-span simply supported reinforced concrete slab with no transverse steel reinforcement, load posted and located on Martin Spring Outer Road in Phelps County, MO. The original construction combined with the presence of very rigid parapets caused the formation of a wide longitudinal crack which resulted in the slab to behave as two separate elements. In order to clarify the behavior of the structure, load tests were performed and a finite element method (FEM) analysis undertaken. The FRP strengthening was designed to avoid further cracking and such that the transverse flexural capacity be higher than the cracking moment. Both FRP techniques were easily implemented and showed satisfactory performance.

Keywords: Bridge, carbon fibers, FEM, fiber reinforced polymers, load test, reinforced concrete, strengthening.

Paolo Casadei, is a PhD candidate in the Department of Civil Engineering at the University of Missouri-Rolla. He received his BS from the University of Bologna, Italy. His research interests include repair of reinforced concrete structures and validation of in-situ diagnostic cyclic load testing. He is a member of ACI, ASCE, and ICRI. He is an EIT in the United States.

Nestore Galati, is a doctoral student in Composite Materials for Civil Engineering at the University of Lecce, Italy, where he received his B.Sc. in Materials Engineering. He got his M.Sc. degree in Engineering Mechanics at the University of Missouri-Rolla. His research interests include repair of masonry and reinforced concrete structures. He is an EIT in the United States.

Renato Parretti, is an ACI member and senior structural engineer with Co-Force America responsible for numerous FRP design projects throughout the world. Mr. Parretti holds a B.S. in Civil Engineering from the University of Florence, Italy. He is a registered PE in Italy, and an EIT in the United States.

Antonio Nanni, is the V & M Jones Professor of Civil Engineering at the University of Missouri-Rolla. He is a registered PE in Italy, FL, PA, MO and OK. He is an active member in the technical committees of ACI (Fellow), ASCE (Fellow), ASTM and TMS. He was the founding Chairman of ACI Committee 440 - FRP Reinforcement and is the current Chairman of ACI Committee 437 - Strength Evaluation of Existing Concrete Structures.

INTRODUCTION

Over 40 percent of the nation's bridges are in need of repair or replacement⁽¹⁾. Budget constraints prohibit many states from repairing or replacing all of these bridges; consequently, states are forced to post load restrictions on their bridges as a temporary solution until more funds become available for repair or replacement. Advanced composite materials made of fiber reinforced polymers (FRP) have a high potential for providing a solution to this problem.

The bridge selected for this project is located on old Route 66, now Martin Springs Outer Road, in Phelps County, Missouri (see Figure 1). This bridge was commissioned in 1926 and was originally on a gravel road. In 1951, the last miles of US Route 66 through Phelps County were concrete paved. In 1972, Route 66 was replaced by interstate I-44. Commissioning of I-44 led to a significant decrease in traffic along Route 66. Load posting of this bridge (a load restriction posting of S-16 trucks over *13 tons (11.79 tons in SI units) 15 mph (24.14 km/hr)*, except for single unit trucks H-20 weight limit to *19 tons (17.24*

tons in SI units), and all other trucks weight limit 30 tons (27.21 tons in SI units)) was approved around 1985 and had a significant impact on the local economy.

This bridge is a three-span simply supported reinforced concrete slab. The total bridge length is 66 ft (20.12 m) and the total width of the deck is 22.5 ft (6.86 m). Figure 2 shows a detailed geometry of the bridge. Based on visual and Non Destructive Testing (NDT) evaluation, it was determined that the superstructure is a solid concrete slab 14 in (35.56 cm) thick, running from pier to pier, the longitudinal reinforcement is made of #8 (25.4 mm) bars spaced at 5 in (12.7 cm). on centers, and no transverse reinforced is present. From cores (cylinders 3 in×6 in, 7.62 cm× 15.24 cm) , the average compressive strength of the concrete was measured to be 4100 psi (28.27 MPa); the yield of the steel was also tested on one bar sample, and resulted to be 32 ksi (220.63 MPa). The lack of transversal reinforcement and the presence of very rigid parapets caused the slab to crack along all three slabs at mid-span. The cracks are approximately 1 in (2.54 cm) wide, and intersect longitudinal bars (see Figure 3). There is no significant cracking in any other portion of the slab and only minor corrosion of the bars crossing the crack.

Given the very good concrete condition of the bridge, the structure was an ideal candidate for strengthening using CFRP composites⁽²⁾⁽³⁾. Two different strengthening schemes were adopted in this project for evaluation purposes, bonded carbon FRP laminates installed by externally wet lay-up and near surface mounted (NSM) rectangular FRP bars.

The paper describes the use of both strengthening techniques.

BRIDGE ANALYSIS

Load Combinations

For the structural analysis of the bridge the ultimate values of bending moments and shear forces are computed by multiplying their nominal values by the dead and live factors and by the impact factor according to AASHTO⁽²⁾ Specifications as shown in Eq.(1):

$$\omega_u = 1.3 [\beta_d D + 1.67(L + I)] \quad (1)$$

where D is the dead load, L is the live load, $\beta_d=1.0$ as per AASHTO¹ Table 3.22.1A, and I (maximum 30%) is the live load impact calculated as follows:

$$I = \frac{50}{L + 125} = \frac{50}{22 + 125} = 0.34 \leq 30\% \quad (2)$$

and $L=22$ ft (6.70 m) represents the span length from center to center of supports.

Design Truck and Design Lanes

Prior to the design of the strengthening, the analysis of the bridge was conducted by considering a HS20-44 truck load (which represents the design truck load as per AASHTO⁽²⁾ Section 3.7.4) having geometrical characteristics and weight properties shown in Figure 4. According to AASHTO⁽²⁾ Section 3.6.3 fractional parts of design lanes shall not be used for roadway widths less than 20ft (6.09 m). As a consequence of these specifications, the loading conditions required to be checked are laid out in Figure 5.

Figure 5a represents the HS20-44 design truck already described in Figure 4. Given the specific bridge geometry, the worst loading scenario is obtained for the minimum spacing of 14.0 ft (4.27 m) between the two rear axles.

The design lane loading condition consists of a load of 640 lbs per linear foot (9.35 kN/m), uniformly distributed in the longitudinal direction with a single concentrated load so placed on the span as to produce maximum stress. The concentrated load and uniform load is considered to be uniformly distributed over a 10'-0" (3.05 m) width on a line normal to the center lane of the lane. The intensity of the concentrated load is represented in Figure 5b for both bending moments and shear forces. This load shall be placed in such positions within the design lane as to produce the maximum stress in the member (as per AASHTO⁽²⁾ Section 3.6).

Slab Analysis

The deck is considered to be a one-way slab, disregarding the contribution of the parapets. For simplicity, the deck has been studied considering the overall width of the transversal cross section.

The dead load was computed considering the self-weight of the concrete slab plus the permanent weight of the top layer of asphalt. The weight of parapets has been computed according to the geometrical properties of Figure 2c and, for simplicity, distributed throughout the width of the slab. Table 1 presents a summary of these values.

Computations for the *design lane* and the design truck load have been carried out and it has been found that the *design truck load* is the controlling loading condition.

For the flexural analysis, the critical loading condition corresponds to the case when the truck has one of its rear axles at the mid-span of the member (see Figure 6). The factored ultimate moment demand is computed for the entire slab in Eq.(3):

$$M_u = \frac{1.3 \times \omega_D L^2}{8} + \frac{1.3 \times 1.67 \times 1.3 \times P_2 L}{4} \quad (3)$$

$$M_u = \frac{1.3(5.99)(22)^2}{8} + \frac{1.3 \times 1.67 \times 1.3 \times (32)(22)}{4} = 493.69k - ft \quad (669.35kN - m) \quad (4)$$

For the shear analysis, the critical loading condition is when one rear axle is closer to one support and the other is *14 ft (4.27 m)* away over the span (see Figure 7). The factored ultimate shear demand is computed for the entire slab in Eq.(5):

$$V_u = \frac{1.3 \times \omega_D L}{2} + 1.3 \times 1.67 \times 1.3 \left(P_2 + P_2 - \frac{P_2(l+x) + P_2 x}{L} \right) \quad (5)$$

$$V_u = \frac{1.3(5.99)(22)}{2} + 1.3 \times 1.67 \times 1.3 \left(32 + 32 - \frac{32(15) + 32(1)}{22} \right) = 200.60 \text{ kip } (892.31 \text{ kN}) \quad (6)$$

The bridge geometry and material properties are reported in Table 2 along with the computed nominal flexural and shear capacities based on conventional RC theory⁽⁵⁾. Since both ϕM_n and ϕV_n are larger than M_u and V_u respectively, no flexural and shear strengthening are required in the longitudinal direction. The cracking moment of a unit strip has been computed (see Eq.(7)) to design a strengthening scheme able to ensure that $\phi M_{n,transv.}$ is larger or equal than the cracking moment.

$$M_{cr} = \frac{7.5 \sqrt{f'_c} I_g}{h/2} = \frac{7.5 \sqrt{4000} (2744)}{7} = 15.5 \text{ k - ft / ft } (21.01 \text{ kN - m / m}) \quad (7)$$

Where I_g represents the gross moment of inertia of the concrete cross section with $b = 12 \text{ in } (30.48 \text{ cm})$ and $h = 14 \text{ in } (35.56 \text{ cm})$.

BRIDGE STRENGTHENING

The strengthening design follows the previous considerations and has the purpose of giving the bridge a moment capacity in the transversal direction equal or greater to the cracking moment computed in Eq.(7), in order to avoid further crack openings and deterioration of the concrete due to water percolation through the cracks.

Two different FRP strengthening techniques have been adopted: (1) externally bonded CFRP laminates installed by manual wet lay-up, and (2) Near-surface mounted CFRP rods embedded in pre-made grooves and bonded in place with an epoxy-based paste. The main difference between these two techniques belongs to the surface preparation necessary before the application of the strengthening that in turn depends upon the conditions of the concrete substrate on which the laminates and bars are bonded.

Before surface preparation for FRP application, the central crack was repaired in order to re-establish material continuity and assure no water percolation through the crack. For this purpose, the crack was sealed using an epoxy-paste and then Casadei, P., Galati, N., Parretti, R., and Nanni, A., "Strengthening of a Bridge Using Two FRP Technologies," Pag.5

injected with a very low viscosity resin as shown in Figure 8a-b. Once the crack had been repaired, FRP have been applied following the design provisions.

The design of both FRP technologies is carried out according to the principles of ACI 440.2R-02⁽⁶⁾ (ACI 440 in the following). The properties of the FRP composite materials used in the design are summarized in Table 3 and Table 4. The reported FRP properties are guaranteed values.

The ϕ factors used to convert nominal values to design capacities are obtained as specified in AASHTO⁽²⁾ for the as-built and from ACI 440 for the strengthened members.

Material properties of the FRP reinforcement reported by manufacturers, such as the ultimate tensile strength, typically do not consider long-term exposure to environmental conditions, and should be considered as initial properties. FRP properties to be used in all design equations are given as follows (ACI 440):

$$\begin{aligned} f_{fu} &= C_E f_{fu}^* \\ \varepsilon_{fu} &= C_E \varepsilon_{fu}^* \end{aligned} \quad (8)$$

where f_{fu} and ε_{fu} are the FRP design tensile strength and ultimate strain considering the environmental reduction factor (C_E) as given in Table 7.1 (ACI 440), and f_{fu}^* and ε_{fu}^* represent the FRP guaranteed tensile strength and ultimate strain as reported by the manufacturer. The FRP design modulus of elasticity is the average value as reported by the manufacturer.

Externally Bonded CFRP Laminates

The material properties of the laminates that have been used are listed on Table 3. The design for externally bonded laminates called for a total of six, 12 in (30.48 cm) wide, single ply CFRP strips overlapping at center span for 10 ft (3.05 m). The strips were evenly spaced over the width of 20 ft (6.09 m) and ran the entire width of the slab, as shown in Figure 9. The moment capacity provided with this strengthening scheme is equal to $\phi M_n = 16.5 \text{ k-ft}$ (23.37 kN-m). The CFRP laminates were applied by a certified contractor in accordance to manufacturer's specification⁽⁹⁾ (see Figure 10).

Near Surface Mounted Rectangular Bars

The material properties of the NSM and epoxy paste that have been used are listed on Table 4. The required number of near-surface mounted reinforcement was determined to be two CRFP tapes per slot on a 9 in (22.86 cm) groove spacing. The bars were embedded in 17 ft (5.18 m) long, $\frac{3}{4}$ in (19.05 mm) deep, and $\frac{1}{4}$ in (6.35 mm) wide grooves cut onto the soffit of the bridge deck as shown in Figure 11. The moment capacity provided with this strengthening scheme is equal to $\phi M_n = 15.5 \text{ k-ft}$ (21.01 kN-m). NSM bars were applied by a certified contractor

following the specifications⁽⁸⁾ prescribed by the University of Missouri - Rolla (see Figure 12).

IN-SITU LOAD TESTING

In order to validate the behavior of the bridge prior and after strengthening, static load tests were performed with a H20 truck (see Figure 13). Although H20 and HS20 trucks differ in their geometry, the loading configuration that maximize the stresses and deflections at mid span could still be accomplished (see Figure 14). Displacements in the longitudinal and transversal direction were measured using eight Linear Variable Differential Transducers (LVDTs) and a data acquisition system under a total of three passes, one central and two laterals. For each pass three stops were executed with the truck having its rear axle centered over the marks on the asphalt (see Figure 15). During each stop, the truck stationed for at least two minutes before proceeding to the next location in order to allow stable readings.

The results of the first load test, relatively to the stop No.3, are reported in Figure 16. All diagrams show the discontinuity caused by the longitudinal crack. The bridge performed well in terms of overall deflection. In fact, the maximum deflection measured during the load test is below the allowable deflection prescribed by AASHTO⁽²⁾ Section 8.9.3 ($d_{max} = L/800 = 0.33in (8.38mm)$).

A second load test was performed after the installation of the FRP materials. The monitoring devices were placed at the same locations of the previous load test.

Test results of the second load test, as expected, show a slight improvement in the deflection of the deck in both the longitudinal and transversal direction (see Figure 17 and Figure 18, respectively).

FEM ANALYSIS

To validate the data obtained from the load tests, a linear elastic FEM analysis was conducted. For this purpose a commercially available finite element program ANSYS 6.1⁽¹¹⁾ was used.

The element SOLID65 was chosen to model the concrete. The SOLID65 element is a brick element defined by eight nodes having three degrees of freedom at each node.

For this project, the material properties of concrete were assumed to be isotropic and linear elastic, since the applied load was relatively low. The modulus of elasticity of the concrete was based on the measured compressive strength of the cores obtained from the slab according to the standard equation ACI 318-02⁽⁵⁾ Section 8.5.1:

$$E_c = 57000\sqrt{f'_c} \approx 3.6 \times 10^6 \text{ psi (24.8 GPa)} \quad (9)$$

Each element was meshed to be $3.5\text{ in}\times 5\text{ in}\times 6\text{ in}$ ($8.9\text{ cm}\times 12.7\text{ cm}\times 15.2\text{ cm}$). In order to take into account the presence of the parapet and curb, an equivalent, less complex shape was chosen. Boundary conditions were simulated as simply supported at both ends (see Figure 19). To take into account the presence of the longitudinal crack, the modulus of elasticity of the central elements was reduced of a thousands times with respect to the value expressed in Eq.(9). From in-situ inspection, the depth and width of the crack was chosen to be equal to one element dimensions. The load was applied on 8 nodes simulating the truck wheels; each force was equal to 4 kip (17.8 kN) for the H20 truck.

The experimental and analytical results for the central and right passes in the transversal direction are reported in Figure 20. The graph shows the good match in deflection between the experimental and analytical results.

Average S_x stresses (stresses in the transversal direction) are plotted in Figure 21, for both the un-cracked and cracked models; they show how the presence of the rigid parapets has a significant effect on the overall behavior of the bridge, justifying the presence of peak horizontal stresses along the slab centerline (tensile stresses are positive) as responsible for the formation of the crack. The strengthening with FRP can overcome these stresses and guarantee a flexural capacity in the transversal direction higher than the cracking moment, blocking new crack's opening.

CONCLUSIONS

The following conclusions can be drawn:

- As a result of FRP strengthening, load posting of the bridge was removed.
- FRP systems either in the form of externally bonded laminates and Near Surface Mounted bars showed to be a feasible solution for the strengthening of the concrete bridge.
- In situ load testing has proven to be useful and convincing.
- The FEM analysis has shown good match with experimental results demonstrating the effectiveness of the strengthening technique.

ACKNOWLEDGEMENTS

Phelps County is the owner of the bridge: its commissioners and staff provided the opportunity and helped in the implementation - Richard Pilcher, MoDOT's Official, and three River Engineers, Springfield, MO, provided oversight.

The authors would like to acknowledge the financial support of the Missouri Department of Transportation, the University Transportation Center (UTC) at the University of Missouri-Rolla (UMR) for the research component of the project.

Master Contractors installed the FRP systems. Hughes Brothers and Master Builders provided the FRP materials, as members of the NSF I/UCRC at UMR.

REFERENCES

- (1) Stone, D.K., Tumialan, J.G., Parretti, R., and Nanni, A., (2002). "Near-Surface Mounted FRP Reinforcement: Application of an Emerging Technology", *Concrete UK*, V. 36, No. 5, pp. 42-44.
- (2) Alkhrdaji, T., Nanni, A., Chen, G., and Barker, M. (1999), "Upgrading the Transportation Infrastructure: Solid RC Decks Strengthened with FRP," *Concrete International*, American Concrete Institute, Vol. 21, No. 10, pp. 37-41.
- (3) Nanni, A., (1997), "Carbon FRP Strengthening: New Technology Becomes Mainstream," *Concrete International: Design and Construction*.
- (4) AASHTO, 2002: "Standard Specifications for Highway Bridges", 17th Edition, Published by the American Association of State Highway and Transportation Officials, Washington D.C.
- (5) ACI 318-02, 2002: "Building Code Requirements for Structural Concrete and Commentary (318R-02)," Published by the American Concrete Institute, Farmington Hills, MI.
- (6) ACI 440.2R-02, 2002: "Guide for the Design and Construction of Externally Bonded FRP Systems for Strengthening Concrete Structures," Published by the American Concrete Institute, Farmington Hills, MI.
- (7) Yang, X., " The engineering of construction specifications for externally bonded FRP composites" Doctoral Dissertation, Department of Civil Engineering, University of Missouri-Rolla, Rolla, Missouri, 2001, 166 pp.
- (8) De Lorenzis, L. (2002), "Strengthening of RC Structures with Near Surface Mounted FRP Rods", Ph.D. Thesis, Department of Innovation Engineering, University of Lecce, Italy, 289 pp.
<http://nt-lab-ambiente.unile.it/delorenzis>
- (9) Watson Bowman Acme Corp. (2002), Wabo[®]MBrace Composite Strengthening System Design Guide, Third Edition, Amherst, New York.
- (10) Hughes Brothers, Inc. (2002), Aslan[®] 500 CFRP Tape,
<http://www.hughesbros.com>
- (11) ANSYS User's Manual for Revision 6.1: Volume I Procedure and Volume III Elements, Swanson Analysis Systems, Inc., 2000.

LIST OF TABLES

Table 1 – Dead Load ($1\text{ k/ft} = 14.7\text{ kN/m}$)

Slab Self-Weight	$\omega_{d1} = (0.15\text{ k} / \text{ft}^3)(270/12\text{ ft})(14/12\text{ ft}) =$	3.94	k/ft
Asphalt Weight	$\omega_{d2} = (0.14\text{ k} / \text{ft}^3)(234/12\text{ ft})(6/12\text{ ft}) =$	1.37	k/ft
Parapet Weight	$\omega_{d3} = (0.15\text{ k} / \text{ft}^3) \left[(326.49/12^2\text{ ft}^2) \times 2 \right] =$	0.68	k/ft
Total Dead Load	$\omega_D = \omega_{d1} + \omega_{d2} + \omega_{d3} =$	5.99	k/ft

Table 2 – Flexural and Shear Capacity

b	h	d	A _s	φM _n	φV _n	M _u	V _u
in [cm]	in [cm]	in [cm]	in ² [cm ²]	k-ft [kN-m]	kip [kN]	k-ft [kN-m]	kip [kN]
270	14	12.75	42.7	1229	370	493.7	200
[685.8]	[35.5]	[32.38]	[275.5]	[1666]	[1646]	[669.3]	[892]

Table 3 – Properties of CFRP Laminate Constituent Materials

Material	Ultimate tensile strength f_{fu}^*	Ultimate strain ϵ_{fu}^*	Tensile modulus E_f	Nominal thickness t_f
	ksi [Mpa]	in/in [mm/mm]	ksi [GPa]	in [mm]
Primer ⁽¹⁾	2.5 [17.2]	40	104 [0.7]	-
Putty ⁽¹⁾	2.2 [15.2]	7.0	260 [1.8]	-
Saturant ⁽¹⁾	8.0 [55.2]	7.0	260 [1.8]	-
High Strength Carbon Fiber ⁽²⁾	550 [3790]	0.017	33,000 [228]	0.0065 [0.1651]

⁽¹⁾ Values provided by the manufacturer ⁽⁹⁾

⁽²⁾ Tested as laminate with properties related to fiber area ⁽⁷⁾

Table 4 – Properties of NSM CFRP Constituent Materials

Material	Ultimate tensile strength f_{fu}^* ksi [MPa]	Ultimate strain ϵ_{fu}^* [in/in]	Tensile modulus E_f ksi [GPa]	Cross Sectional Area in ² [mm ²]	Dimen- sions in×in [mm×mm]
Concresive 1420 Epoxy ⁽¹⁾	4 [27.58]	0.1	-	-	-
Aslan 500 Carbon Tape ⁽²⁾	300 [2,068]	0.017	19000 [131]	0.05 [32.2]	0.079×0.63 [2×16]

⁽¹⁾ Values provided by the manufacturer ⁽⁹⁾

⁽²⁾ Values provided by the manufacturer and related to cross sectional area ⁽⁹⁾

LIST OF FIGURES



Figure 1 – Martin Spring Bridge

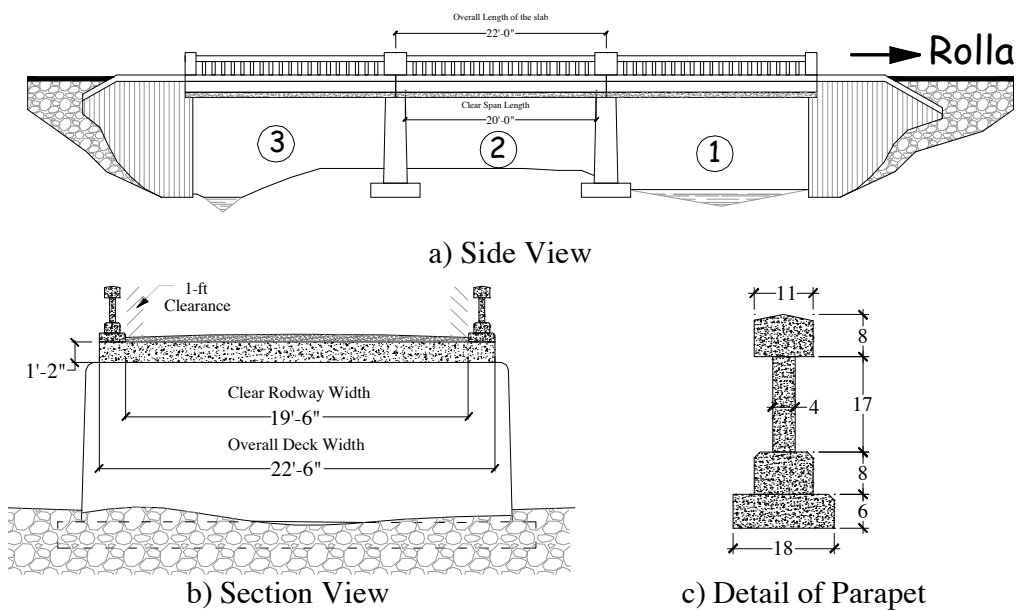


Figure 2 –Martin Spring Bridge Geometry (US units; 1 in =2.54 cm)



Figure 3 – Soffit Slab Longitudinal Crack

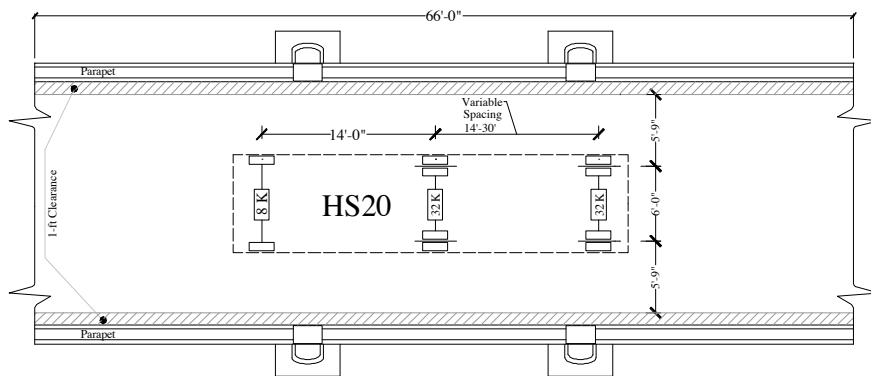
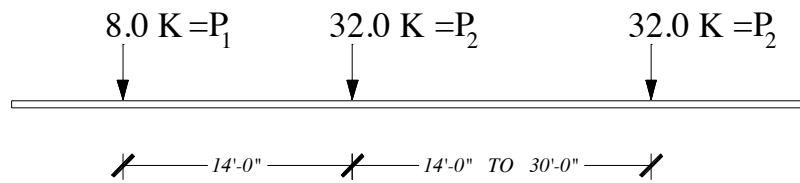
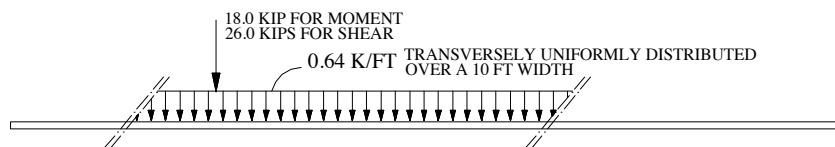


Figure 4 – Truck Load and Truck Lanes
(US units; 1 kip= 4.45 kN; 1 ft =30.48 cm)



a) Design Truck (HS20-44)



b) Design Lane

Figure 5 – Loading Conditions (US units; 1 kip= 4.45 kN; 1 ft =30.48 cm)

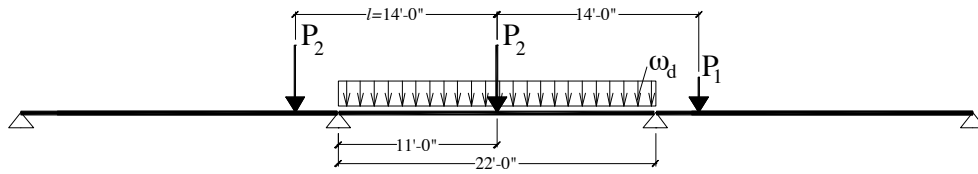


Figure 6 – Flexural Design Configuration (US units; $l_{ft} = 30.48cm$)

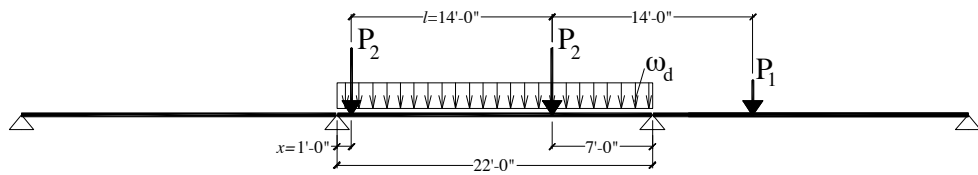
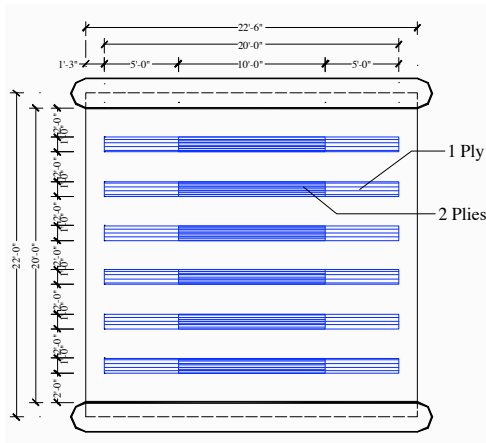


Figure 7 – Shear Design Configuration (US units; $l_{ft} = 30.48cm$)

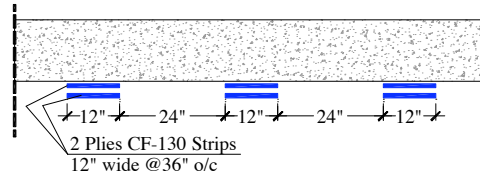


a) Crack Sealed Previous to Injection b) Crack Injection under the Bridge

Figure 8 – Repair of Central Crack



a) Plan View



b) Section View

Figure 9 – Strengthening with Laminates on Span 1 and 3
(US units; $1in = 2.54cm$)



a) Surface Preparation with Primer and Putty



b) Application of Saturant



c) Application of CFRP Laminates



d) Application Completed

Figure 10 – Phases of CFRP Laminate Application

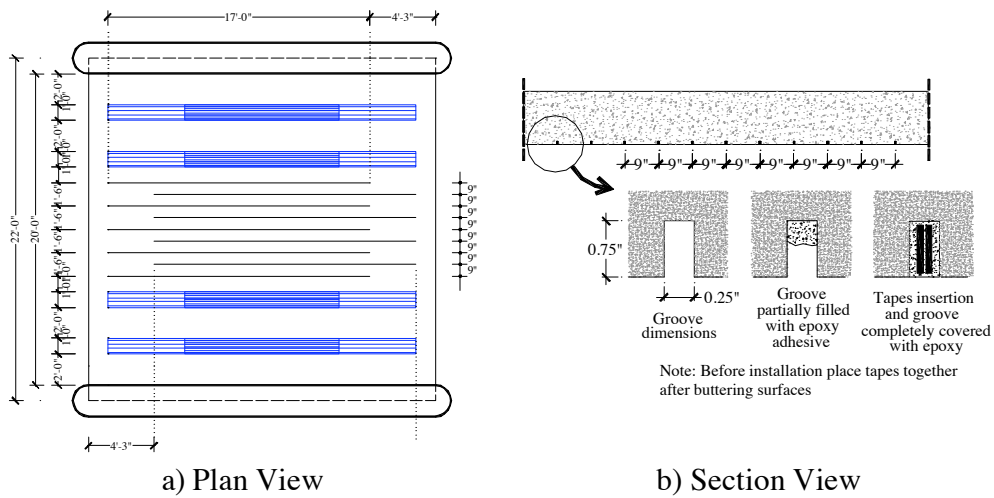


Figure 11 – Strengthening with NSM Bars and CFRP Laminate on Span 2
(US units; $1in= 2.54cm$)

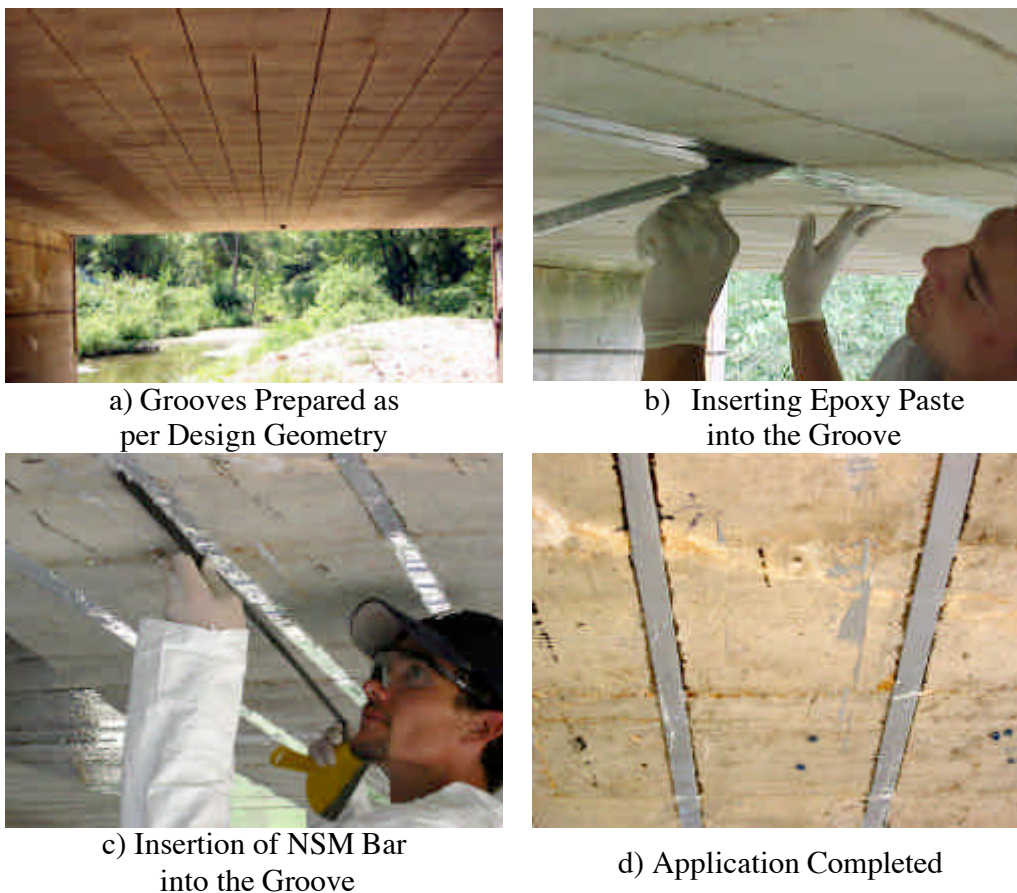


Figure 12 – Phases of NSM Bar Application



Figure 13 – Load Test with H20 Truck

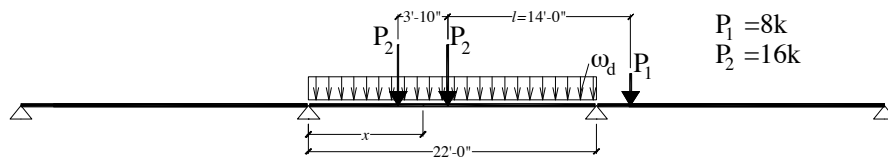
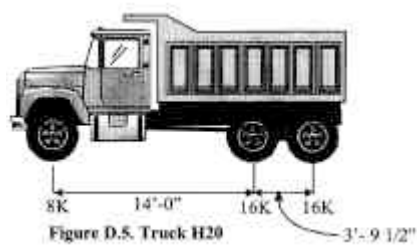


Figure 14 – H20 Legal Truck (US units; $1 \text{ kip} = 4.45 \text{ kN}$; $1 \text{ ft} = 30.48 \text{ cm}$)

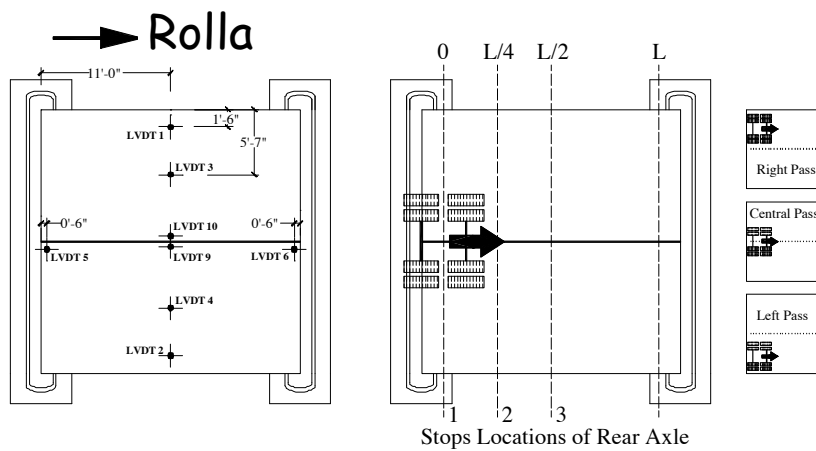


Figure 15 – LVDTs Positions and Truck Stops

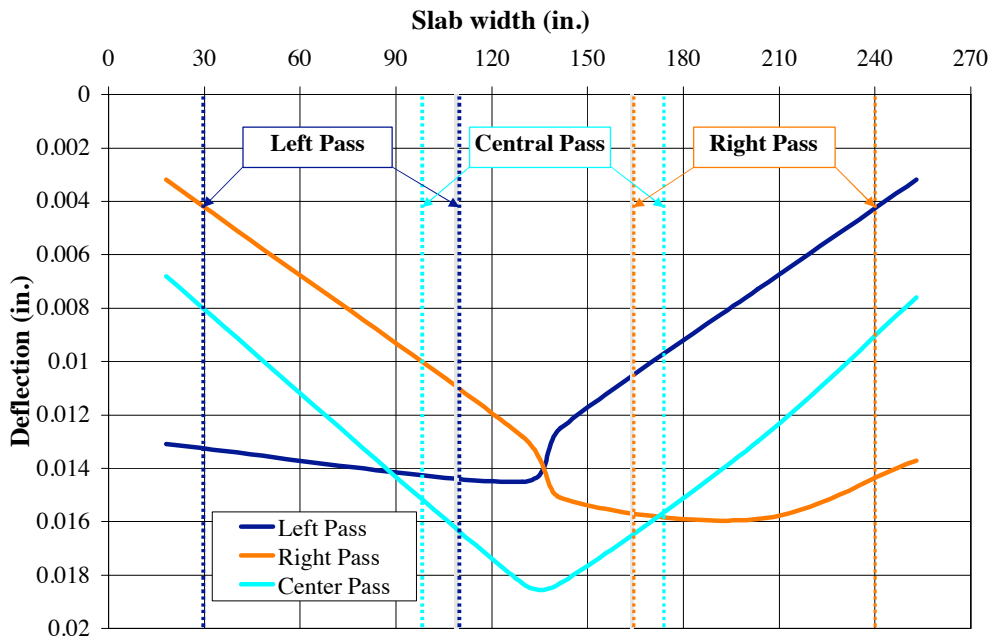


Figure 16 – Mid Span Deflection in the Transverse Direction, Stop No.3
(US units; $1in= 2.54cm$)

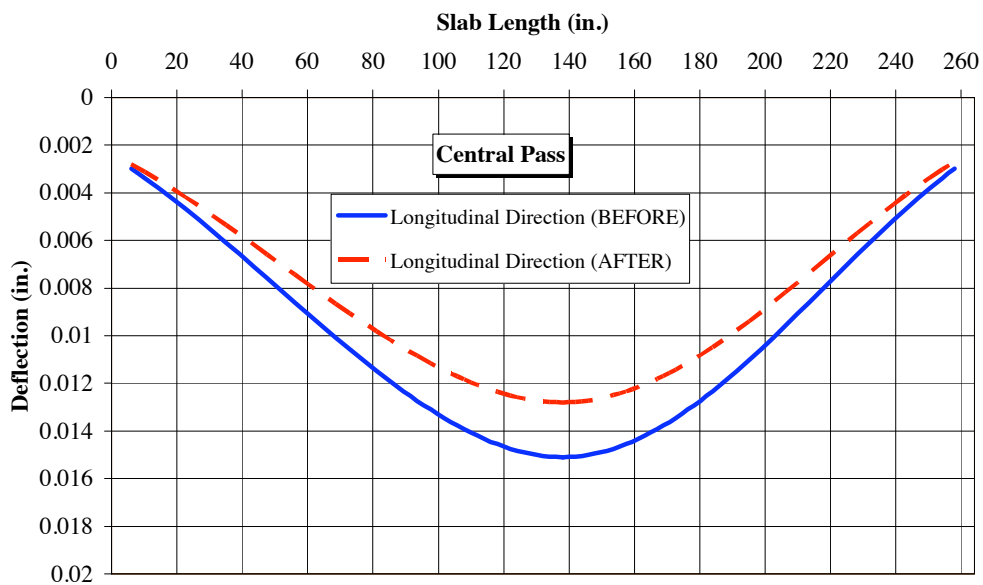


Figure 17 – Center Line Deflection in the Longitudinal Direction, Stop No.3
(US units; $1in= 2.54cm$)

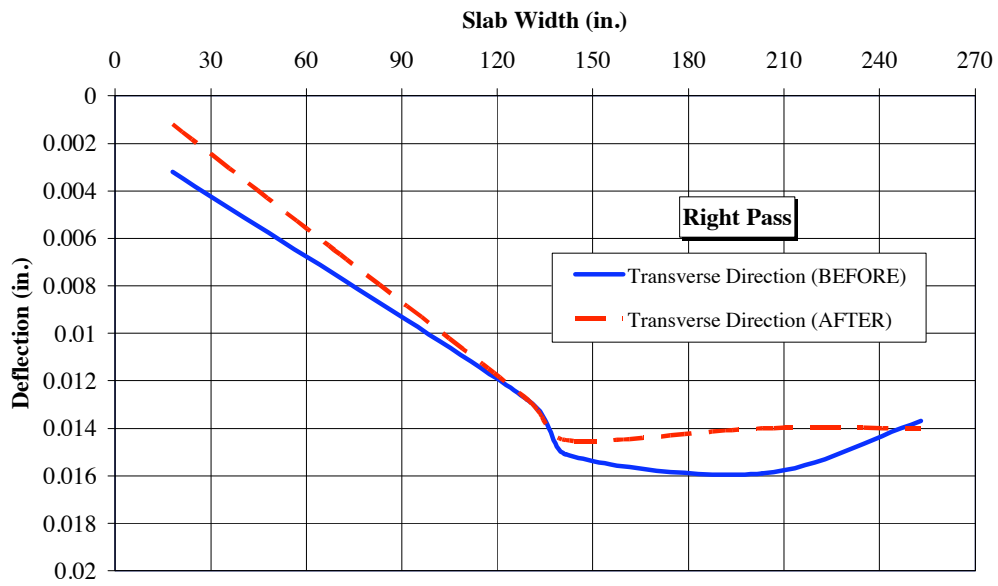
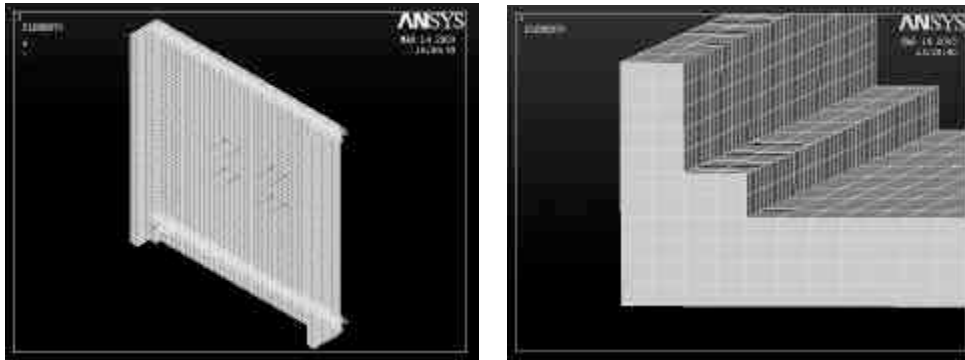


Figure 18 – Mid Span Deflection in the Transverse Direction, Stop No.3
(US units; $1in = 2.54cm$)



a) Entire Model

b) Detail of Parapet

Figure 19 – FEM Model Geometry

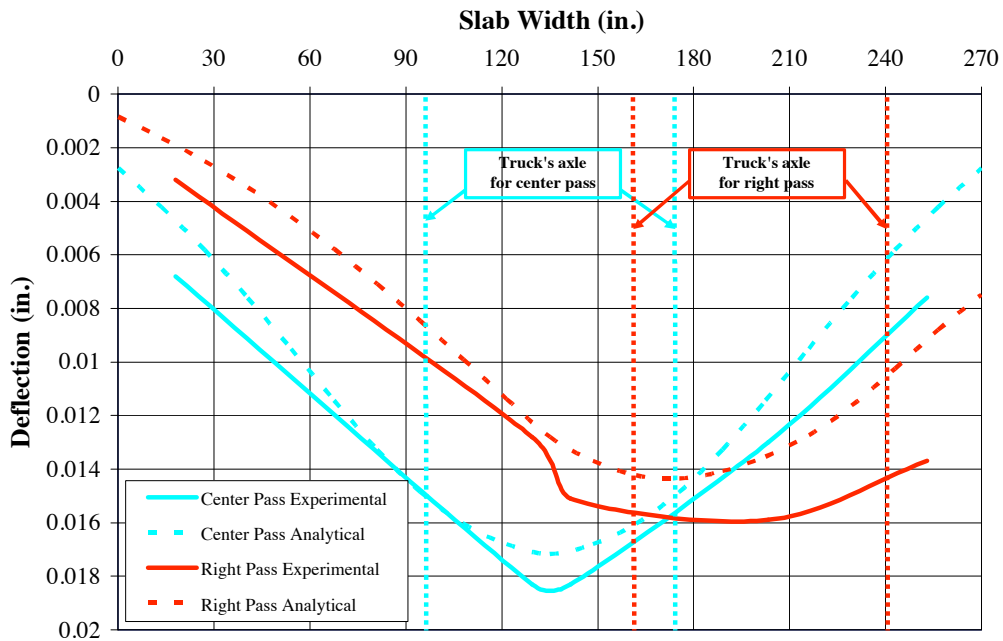
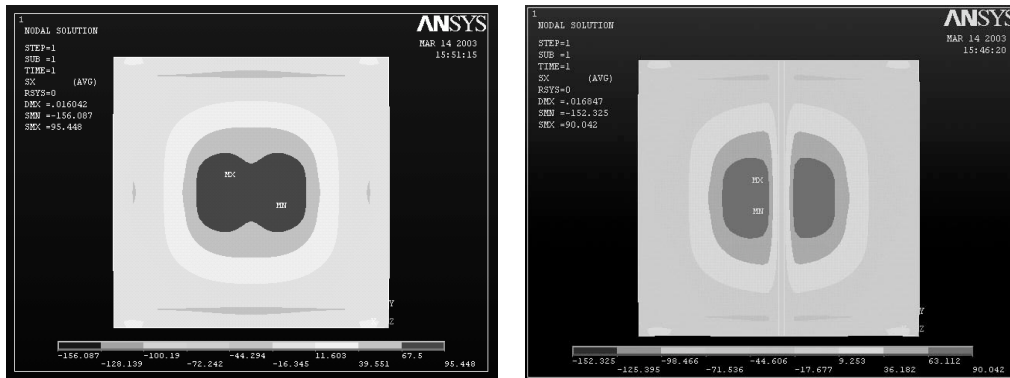


Figure 20 – Comparison of Experimental and Analytical Results in the Transversal Direction (US units; $1in= 2.54cm$)



a) S_x in Model Slab with no Crack

b) S_x in Model Slab with Crack

Figure 21 – FEM Results of S_x Average Stresses for Axle Position at Stop 3 (vertical direction in diagram corresponds to longitudinal direction in the bridge)